

Atomic and Electronic Structure of Mixed and Partial Dislocations in GaN

Ilke Arslan,¹ Andrew Bleloch,² Eric A. Stach,^{3,4} and Nigel D. Browning^{3,5}

¹*Department of Materials Science and Metallurgy, University of Cambridge, Pembroke Street, Cambridge CB2 3QZ, United Kingdom*

²*UK SuperSTEM, Daresbury Laboratory, Daresbury, Cheshire WA4 4AD, United Kingdom*

³*National Center for Electron Microscopy, Lawrence Berkeley National Laboratory,
One Cyclotron Road, Berkeley, California 94720, USA*

⁴*School of Materials Engineering, Purdue University, West Lafayette, Indiana 47907 USA*

⁵*Department of Chemical Engineering and Materials Science, University of California–Davis, Davis, California 95616, USA*

(Received 20 July 2004; published 20 January 2005)

Here we present a detailed study of mixed dislocations in GaN, in which the complexities of the atomic arrangement in the cores have been imaged directly for the first time using an aberration corrected scanning transmission electron microscope. In addition to being present as a full-core structure, the mixed dislocation is observed to dissociate into partial dislocations separated by a stacking fault only a few unit cells in length. The generation of this stacking fault appears to be impurity driven and its presence is consistent with theoretical predictions for dislocation dissociation in materials with hexagonal crystal symmetry.

DOI: 10.1103/PhysRevLett.94.025504

PACS numbers: 61.72.Ff, 68.37.Lp

The wide band-gap semiconductor gallium nitride (GaN) and its alloys have received tremendous attention in recent years due to its applications in light emitting diodes and laser diodes in the blue region of the spectrum [1,2]. One major area of research involves understanding the influence of the abundant dislocations present in the active layer of devices on the efficiency of the optical response and the long-term device reliability [3]. Of particular interest from both the technological and fundamental scientific perspectives is that devices operate despite dislocation densities far in excess of other optoelectronic materials [4]. However, while the devices do function, dislocations ultimately appear to control device performance (overall efficiency, lifetime, etc.) and actually limit the electron mobility in field-effect transistor and high electron mobility transistor devices [5]. Therefore, they need to be wholly understood for the benefits of efficient optical devices based on GaN alloys to be fully realized [3].

To some extent, the limitation in the understanding of dislocation mechanisms in GaN originates from the hexagonal nature of the wurtzite crystal structure. The vast majority of our understanding of dislocations is based on cubic materials. Our understanding of dislocation behavior in hexagonal materials is substantially less complete, although there have been numerous proposed models for these systems [6–10]. This lack of a completely defined picture for dislocations in hexagonal materials has in part led to the great debate about the fundamental role of the dislocations in GaN. For example, edge- and screw-type dislocations have been studied to a great extent by many research groups. In the [0001] orientation, the atomic structure of the edge dislocation has been shown to have a full, eight-atom core both experimentally [11] and theoretically [12]. Although this structure is calculated to have the lowest energy for the edge dislocation, evidence exists

for other structures such as the four-atom structure and five- or seven-atom structure [13]. Additionally, several different atomic core structures have been shown to exist experimentally for the screw dislocation, namely, full core, filled core, and open core [14,15], which have been confirmed theoretically [12,16]. In this case it is the open core dislocation with diameter ~ 7.2 Å that appears to have the lowest energy structure.

The effect of these cores' structures on the electronic properties of the edge and screw dislocations is also under some debate. Experimentally, there is atomic scale evidence [11,14] that intrinsic dislocations are electrically inactive, although lower spatial resolution studies indicate some level of localized states [17]. Similarly, there is theoretical evidence both that the intrinsic dislocations are [18] and are not [12,19] electrically active. Electron holography and scanning capacitance experiments [20,21] show that edge dislocations are negatively charged, while another holography experiment shows that all three types of dislocations are negatively charged in *n*-type materials [22]. Furthermore, a reverse-bias leakage study showed that pure screw dislocations are far more detrimental than edge or mixed dislocations and that this may be attributed to their electrical activity [23].

These apparent discrepancies in the literature appear mainly to arise from the difficulties in separating effects due to intrinsic dislocations from those due to the interaction of impurities and other defects with the dislocations [14,24,25]. To fully understand the effect of dislocations we therefore need to investigate the effects of the impurities on the dislocation core structures and the subsequent electronic properties. One of the best ways to achieve this is to investigate defect impurity interactions on the atomic scale. In this Letter, we discuss results obtained from mixed dislocations in GaN that shed new light on these

defect interactions and also provide an experimental verification of proposed models of partial splitting of dislocations in hexagonal materials. Experimentally, very little work has been performed on mixed dislocations as the lack of spatial resolution in standard electron microscopes, small signal levels, and the local plane bending makes them difficult to image. Computationally, the combination of edge and screw Burgers vectors are very demanding on computer time due to the large distortions in the core structure, and many computational system sizes today still cannot accommodate them.

The ability to now image mixed dislocation cores in GaN has arisen through advances in aberration correction of dedicated scanning transmission electron microscopes (STEM) that have demonstrated spatial resolution of ~ 1 Å [26]. The microscopy in this Letter was performed at the UK superSTEM laboratory on a VG HB501 dedicated STEM fitted with a Nion second generation spherical aberration corrector and a Gatan Enfina electron-energy loss spectrometer. The convergence semiangle of the electron probe was 24 mrad for both imaging and spectroscopy. The collection semiangle for the electron-energy-loss spectroscopy (EELS) spectra was 15 mrad and for the high angle annular dark field imaging was 70 to 200 mrad.

The samples analyzed in this study are metal-organic chemical vapor deposition grown on sapphire substrates. They are *n*-type doped materials, with an approximate Si-dopant concentration of 5×10^{17} . From superSTEM images of ~ 50 mixed dislocations, the core structure of the undissociated mixed dislocation was determined to be an eight-atom ring core, just like the edge dislocation [11]. Figure 1(a) shows a raw Z-contrast image showing this atomic structure. It should be noted that all images presented in this Letter are unprocessed images unless otherwise stated. Because of the incoherent nature of Z-contrast images [27], the atomic structure can be obtained directly from this image without the necessity of image simulations. It is possible to distinguish this dislocation from edge dislocations due to the large amount of strain present from its screw component. Figure 1(b) shows a ball and stick model derived directly from Fig. 1(a), showing the atomic structure more clearly. To some extent, this result was anticipated because the mixed dislocation should be a linear combination of the screw and edge components, which means that the edge component should be an eight-atom ring core, but it has not been verified experimentally to be so until now.

The level of strain (and large Burgers vector) present at mixed dislocations is generally not favorable in crystals, and it might be expected that it would structurally reorder to reduce its energy. Figure 2(a) shows a mixed dislocation that has split into two partial dislocations with a stacking fault structure in between. This stacking fault lies along the $[\bar{1}100]$ direction and in the $(11\bar{2}0)$ habit plane (i.e., the *a* plane). This separation of dislocations into partials sepa-

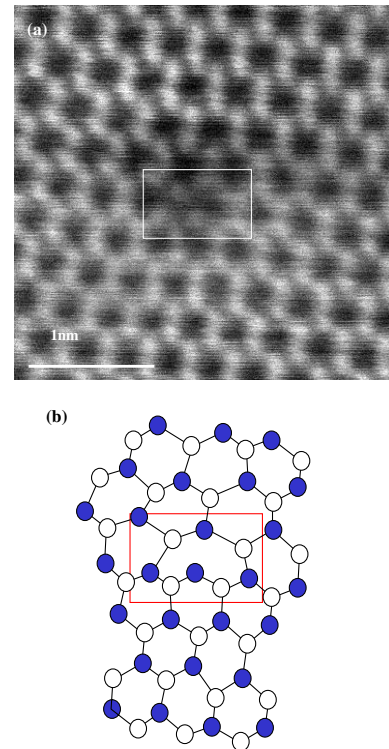


FIG. 1 (color online). Z-contrast image of a full-core mixed dislocation, with the core outlined in the box (a), and a ball and stick model of the eight-atom ring atomic structure (b).

rated by a stacking fault is known to occur in many other materials [9] but has never been observed on the atomic scale in materials with hexagonal crystal symmetry, such as GaN. As can be seen from the image, the large amount of strain that made it difficult to image many of the cores of the mixed dislocations is not present here. While there is still strain observed, the ability to image individual atomic columns strongly suggests that the dissociation of the dislocation into partials has reduced the net strain energy in the dissociated core structures. The structure of the core appears to be a screw dislocation at the left end (which is usually seen as a six-atom ring) and an edge dislocation at the right end (which is usually an eight-atom ring) with a stacking fault between the two [28]. The screw component causes a distortion in the *c* direction, which gradually decreases as the stacking fault widens to accommodate the strain of the edge component with the insertion of an extra plane of atoms. It should be noted that there have been other types of stacking faults observed in GaN to lie on the *a* plane, namely, those with $\{R\} = \frac{1}{2}\langle 10\bar{1}1 \rangle$ and $\{R\} = \frac{1}{6}\langle 20\bar{2}3 \rangle$ displacement vectors [29]. However, the geometries of these stacking faults are different from the one we present here, and the partial dislocations that terminate these stacking faults have not been imaged to date.

The assignment of these features as edge, screw, and stacking fault can be confirmed by EELS [27]. Figure 3 shows a series of spectra from various parts of the partial

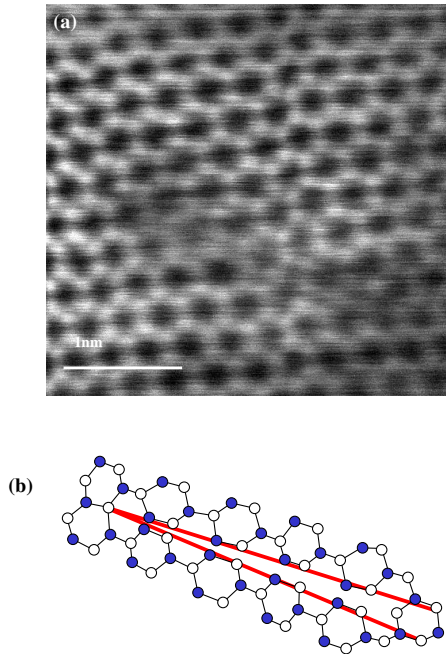


FIG. 2 (color online). Z-contrast image of a dissociated mixed dislocation, showing a stacking fault in between the edge and screw dislocation cores (a). The ball and stick model (b) clarifies the atomic structure and shows how the stacking fault widens in the plane of the image between the two dislocations to accommodate the strains associated with each dislocation. Other similar partial dislocations connected by stacking faults have been observed with the lengths of the stacking faults extending over $\sim 15\text{--}30$ Å in length.

dislocation compared to a bulk spectrum away from the dislocation. The spectrum that was taken from the nine-atom ring (on the right terminating side) shows a fine structure that is very similar to that of the bulk, while the

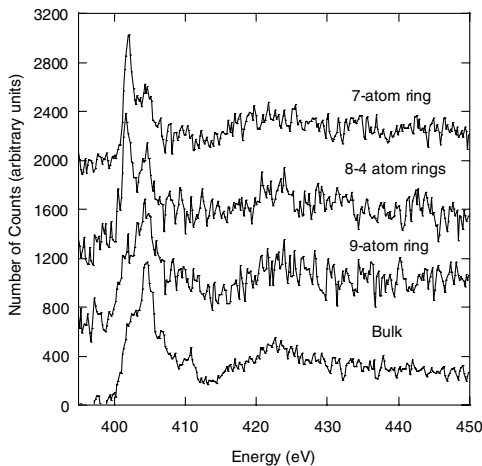


FIG. 3. Electron-energy loss spectra from the partial dislocation, compared to bulk GaN. The fine structure of the N K -edge confirms that one dislocation has a screw character while the other has an edge character.

spectra from the 8-4 atom rings in the stacking fault and the seven-atom ring (on the left terminating side) show a fine structure that is dramatically different. Based on the previous results and analysis of the other two types of dislocation cores [11,19], we can see that this change in fine structure is related to the screw component of the mixed dislocation. The similar fine structure to the bulk (in the nine-atom ring) was observed in the edge dislocation [11,19]. The 8-4 atom rings also contain distortions in the c direction and so exhibit a fine structure consistent with the screw dislocation. This comparison suggests that when the mixed dislocation dissociates, one side of the partial maintains the perfect edge component of the mixed dislocation, while the other side of the partial maintains the perfect screw component of the mixed dislocation.

Because of the two-dimensional nature of the imaging, it is possible to determine the Burgers vector of the partial dislocations only in one direction, which is not sufficient to fully characterize these dislocations as they also have components in the c direction (into the page). Further, as we discussed earlier, because GaN is a hexagonal close-packed structure, there are too many variables to be able to determine the slip plane on which these stacking faults in the partial dislocations form. To obtain the necessary information to be able to answer these questions, an experiment was performed using conventional TEM weak beam dark field imaging [30]. However, the results of this experiment did not yield any distinction between normal mixed dislocations and dissociated mixed dislocations because the resolution of the weak beam dark field technique was not sufficient to be able to distinguish the small separation of $15\text{--}30$ Å. The next step in the understanding of the slip planes on which they form, their Burgers vector, etc., must come from either density functional theory calculations or an *in situ* straining experiment.

However, we can gain some understanding of the dissociation mechanism from standard models for hexagonal close-packed materials. The four different dissociation reactions that have been postulated for the hexagonal close-packed structure [4,6,7,10] are summarized below:

$$\text{Case A: } \frac{1}{3}[11\bar{2}3] \rightarrow \frac{1}{3}[11\bar{2}0] + [0001] + SF_{(1\bar{1}00)},$$

$$\text{Case B: } \frac{1}{3}[11\bar{2}3] \rightarrow \frac{1}{6}[20\bar{2}3] + \frac{1}{6}[02\bar{2}3] + SF_{(11\bar{2}2)},$$

$$\text{Case C: } \frac{1}{3}[11\bar{2}3] \rightarrow \frac{1}{3}[10\bar{1}0] + \frac{1}{3}[01\bar{1}3] + SF_{(0001)},$$

$$\text{Case D: } \frac{1}{3}[11\bar{2}3] \rightarrow \eta \frac{1}{3}[11\bar{2}3] + \frac{1-\eta}{3}[01\bar{1}3] + SF_{(11\bar{2}2)}.$$

Of these four different dissociation pathways, the image and spectra allow us to identify case A as being present in the dissociation of the mixed dislocation in GaN. This is the only mechanism consistent with the dissociation into a

pure edge and pure screw. All other dissociations yield stacking faults that lie on planes that do not match the images. What is interesting is that there is no apparent energy savings in the simple dissociation of $\langle a + c \rangle \rightarrow \langle a \rangle + \langle c \rangle + SF$. In fact, to first order, the stacking fault increases the total energy of the configuration. Therefore, a possible cause for this split into partial dislocations may arise from the segregation of point defects and impurities to the dislocation. Point defect and impurity segregation have been observed in other studies of dislocation cores in GaN [14,15]. It is conceivable that point defects or impurities could segregate preferentially to either the edge or screw kink configurations along the mixed dislocation core during crystal growth, making the separation of the total mixed dislocation into two partials and a stacking fault an energetically acceptable manner to locally relieve lattice strain associated with this segregation.

In conclusion, we have observed the local atomic and electronic structures of full-core and partial mixed dislocations in GaN for the first time. The full-core mixed dislocation has the same eight-atom core structure in the [0001] orientation as that of the edge dislocation, and the mixed partial dislocation dissociates into pure edge and screw dislocations, separated by a narrow stacking fault, as established through EELS analyses and proposed dissociation considerations. This dissociation is attributed to the segregation of impurities and/or point defects to the dislocation cores. In terms of optical properties, the formation of the extended defect structure in the dissociated cores may have a dramatic effect on the efficiency of the devices. This combination of atomic resolution imaging and spectroscopy provides an excellent guide to future atomistic studies of these same defects to elucidate the formation mechanism and effect on electrical and mechanical properties.

This work was supported by the Director, Office of Science, Office of Basic Energy Sciences, of the U.S. Department of Energy under Contract No. DE-AC03-76SF00098 and Grant No. DE-FG02-03ER46057. The authors also thank C. Kisielowski and C.-Y. Song for sample preparation.

-
- [1] S. Nakamura, T. Mukai, and M. Senoh, *Appl. Phys. Lett.* **64**, 1687 (1994).
 - [2] S. Nakamura, N. Iwasa, M. Senoh, S. Nagahama, T. Yamada, and T. Mukai, *Jpn. J. Appl. Phys. Lett.* **34**, L1332 (1995).
 - [3] S. Nakamura, *Science* **281**, 956 (1998).
 - [4] S.D. Lester, F.A. Ponce, M.G. Craford, and D.A. Steigerwald, *Appl. Phys. Lett.* **66**, 1249 (1995).
 - [5] D.C. Look and J.R. Sizelove, *Phys. Rev. Lett.* **82**, 1237 (1999).

- [6] A. Berghezan, A. Fourdeux, and S. Amelinckx, *Acta Metall.* **9**, 464 (1961).
- [7] J.R. Morris, K.M. Ho, K.Y. Chen, G. Rengarajan, and M.H. Yoo, *Modell. Simul. Mater. Sci. Eng.* **8**, 25 (2000).
- [8] S. Ando, T. Gotoh, and H. Tonda, *Metal. Mater. Trans.* **33A**, 823 (2002).
- [9] J.P. Hirth and J. Lothe, *Theory of Dislocations* (John Wiley, New York, 1982), 2nd ed.
- [10] S.R. Agnew, J.A. Horton, and M.H. Yoo, *Metal. Mater. Trans.* **33A**, 851 (2002).
- [11] Y. Xin, E.M. James, I. Arslan, S. Sivananthan, N.D. Browning, S.J. Pennycook, F. Omnès, B. Beaumont, J.P. Faurie, and P. Gibart, *Appl. Phys. Lett.* **76**, 466 (2000).
- [12] J. Elsner, R. Jones, P.K. Sitch, V.D. Porezag, M. Elstner, Th. Frauenheim, M.I. Heggie, S. Oberg, and P.R. Briddon, *Phys. Rev. Lett.* **79**, 3672 (1997).
- [13] A. Bere and A. Serra, *Phys. Rev. B* **65**, 205323 (2002).
- [14] I. Arslan and N.D. Browning, *Phys. Rev. Lett.* **91**, 165501 (2003).
- [15] Z. Liliental-Weber, Y. Chen, S. Ruvimov, and J. Washburn, *Phys. Rev. Lett.* **79**, 2835 (1997).
- [16] J.E. Northrup, *Phys. Rev. B* **66**, 045204 (2002).
- [17] A. Gutierrez-Sosa, U. Bangert, A.J. Harvey, C. Fall, and R. Jones, *Diam. Relat. Mater.* **12**, 1108 (2003).
- [18] C.J. Fall, R. Jones, P.R. Briddon, A.T. Blumenau, T. Frauenheim, and M.I. Heggie, *Phys. Rev. B* **65**, 245304 (2002).
- [19] I. Arslan and N.D. Browning, *Phys. Rev. B* **65**, 075310 (2002).
- [20] D. Cherns and C.G. Jiao, *Phys. Rev. Lett.* **87**, 205504 (2001).
- [21] P.J. Hansen, Y.E. Strausser, A.N. Erickson, E.J. Tarsa, P. Kozodoy, E.G. Brazel, J.P. Ibbetson, U. Mishra, V. Narayanamurti, S.P. DenBaars, and J.S. Speck, *Appl. Phys. Lett.* **72**, 2247 (1998).
- [22] J. Cai and F.A. Ponce, *Phys. Status Solidi A* **192**, 407 (2002).
- [23] J. Hsu, M.J. Manfra, R.J. Molnar, B. Heying, and J.S. Speck, *Appl. Phys. Lett.* **81**, 79 (2002).
- [24] A. Krtschil, A. Dadgar, and A. Krost, *Appl. Phys. Lett.* **82**, 2263 (2003).
- [25] J. Elsner, R. Jones, M.I. Heggie, P.K. Sitch, M. Haugk, T. Frauenheim, S. Oberg, and P.R. Briddon, *Phys. Rev. B* **58**, 12 571 (1998).
- [26] P.E. Batson, N. Delby, and O.L. Krivanek, *Nature (London)* **418**, 617 (2002).
- [27] N.D. Browning, M.F. Chisholm, and S.J. Pennycook, *Nature (London)* **366**, 143 (1993).
- [28] J.E. Northrup, *Appl. Phys. Lett.* **72**, 2316 (1998).
- [29] P. Vermaut, G. Nouet, and P. Ruterana, *Appl. Phys. Lett.* **74**, 694 (1999).
- [30] D.J.H. Cockayne, in *Electron Microscopy, Diffraction and Imaging Techniques in Materials Science Vol. I*, edited by S. Amelinckx *et al.* (North-Holland, Amsterdam, 1978), p. 153.